Temperature and Frequency Dependence of Magnetic Losses in Fe-Co

IEEE Access
Multidisciplinary | Rapid Review | Open Access Journal

IEEE MAGNETICS SOCIETY SECTION

Received 22 September 2023, accepted 5 October 2023, date of publication 9 October 2023, date of current version 13 October 2023.

Digital Object Identifier 10.1109/ACCESS.2023.3322941

RESEARCH ARTICLE

Temperature and Frequency Dependence of Magnetic Losses in Fe-Co

NICOLETA BANU[1], ENZO FERRARA[1], MASSIMO PASQUALE[1], (Senior Member, IEEE), FAUSTO FIORILLO[1], OLIVIER DE LA BARRIÈRE[2], DANIEL BRUNT[3], ADAM WILSON[3], AND STUART HARMON[3]

[1]Advanced Materials Metrology and Life Sciences Division, Istituto Nazionale di Ricerca-Metrologica (INRIM), 10135 Turin, Italy
[2]Laboratoire SATIE, CNRS—ENS Paris-Saclay, 91190 Gif sur Yvette, France
[3]National Physical Laboratory, TW11 0LW Teddington, U.K.

Corresponding author: Massimo Pasquale (m.pasquale@inrim.it)

This work was supported in part by the Project 19ENG06 HEFMAG, and in part by the European Metrology Programme for Innovation and Research (EMPIR) Programme co-financed by the Participating States and from the European Union's Horizon 2020 Research and Innovation Programme.

ABSTRACT We investigate the temperature dependence of the energy loss $W(f)$ of 0.10 and 0.20 mm thick Fe-Co-V sheets (Vacoflux®and Vacodur®) in the range $-50\ °C \leq T \leq 155\ °C$. The measurements, performed from DC to $f = 5$ kHz on ring samples and Epstein strips, show that $W(f)$ passes through a minimum value around room temperature at all tested polarization values ($1.0 \leq J_p \leq 1.9$ T). The largest effect occurs under quasi-static regime and declines with frequency, depending on the sheet thickness and the ensuing role of the dynamic loss. The somewhat abnormal increase of the quasi-static loss W_{hyst} with temperature, which contrasts with a concurrent decrease of the magnetocrystalline anisotropy constant, is interpreted in terms of temperature-dependent internal stresses and their change with T. The stresses are assumed to derive from the different thermal expansion coefficients of the ordered and disordered structural phases, a conclusion made plausible by the highly magnetostrictive properties of the material, dwelling in a low anisotropy environment. The AC properties are treated by adapting the loss decomposition to the inception and development of a non-uniform induction profile across the sheet thickness (skin effect) at high frequencies. The classical loss component is calculated via the numerical solution of the Maxwell's diffusion equation, where the magnetic constitutive equation of the material is identified with the normal magnetization curve. It turns out that the so-found $W_{class}(f)$ and the resulting excess loss $W_{exc}(f)$ are moderately dependent on temperature and $W(f)$ eventually tends towards a slow monotonical decrease with T at the highest frequencies.

INDEX TERMS Fe-Co alloys, magnetic energy loss, temperature, skin effect, soft magnetic materials.

I. INTRODUCTION

The high values of saturation polarization and Curie temperature of the $Fe_{49}Co_{49}V_2$ alloys, combined with excellent soft magnetic behavior and acceptable mechanical properties, make them the material of choice for many specialized applications in the automotive and aviation industry [1], [2], where the material performances make it economically viable, despite its costs. In all these applications (e.g. high-speed motors, medium-to-high-frequency transformers) one is inevitably confronted with the role of the core temperature, either because of the specific working environment [3] or due to heat generation by the losses.

There is limited experimental evidence regarding the temperature dependence of the magnetic properties of the Fe-Co alloys, probably motivated by the assumption that, at least under ordinary exciting regimes, this dependence is weak and that aging may play a role, thereby hindering definite conclusions. For example, the quasi-static loss measured by Pandey, et al. on Permendur and Supermendur toroidal samples, subjected to a same long-duration annealing at 450 °C, exhibited opposite trends under increasing temperature T,

The associate editor coordinating the review of this manuscript and approving it for publication was Montserrat Rivas.

the hysteresis loss decreasing in the former and increasing in the latter under increasing T [3]. Fingers, et al. have measured the power loss at frequency $f = 1$ kHz and peak magnetic polarization value (maximum value of the magnetic polarization attained under alternating field) $J_p = 1.8$ T in Hiperco 50 ($Fe_{49.3}Co_{48.75}V_{1.9}Nb_{0.05}$), to find a very slight decrease going from room temperature to 200 °C [4]. A larger decrease is found after 2000-hour aging at 500 °C, starting, however, from an aging-induced enhanced loss figure. It is verified that such deterioration is largely caused by the formation of γ_2 precipitates [5], [6]. On the other hand, little analysis of the AC losses and their frequency dependence, so far limited to room temperature, is available at present. The loss decomposition has been investigated up to 150 Hz on 0.10 mm thick $Fe_{49}Co_{49}V_2$ sheets in [7] and is shown to favorably compare with the results on Fe-Si sheet having the same thickness. The limited frequency range covered in these measurements has been overcome in [8], where the loss measured on 0.20 mm thick Vacoflux sheets up to 10 kHz has been modeled by application of the Dynamic Preisach Model. A simpler approach is followed in this work, where recourse will be made to the normal magnetization curve, taken as the constitutive equation of the material, in the treatment of the Maxwell's electromagnetic diffusion equation. The decomposition of the measured energy loss $W(f)$ is thereby obtained for the 0.20 mm and 0.10 mm thick Vacoflux and Vacodur samples up to 2 – 5 kHz. It is concluded that a temperature variation, here spanning between – 50 °C and 155 °C, mainly affects the quasi-static ($f \to 0$) loss W_{hyst}, which passes through a shallow minimum around room temperature. The classical eddy current loss $W_{class}(f)$ eventually overcomes the hysteresis W_{hyst} and the (dynamic) excess loss $W_{exc}(f)$ components in the 0.20 mm thick Vacoflux sheets upon attaining the kHz range, weakening the dependence of $W(f)$ with T, whereas a relatively minor change is observed in the harder and thinner ($d = 0.10$ mm) Vacodur samples.

A rationale for the T dependence of W_{hyst}, W_{class}, and W_{exc} will be discussed in the following (Section III), where the large advantage brought about by a reduced sheet thickness (0.10 mm vs. 0.20 mm) in the kHz range, caused by a correspondingly reduced $W_{class}(f)$ and $W_{exc}(f)$ figures, will be highlighted.

II. EXPERIMENTAL PROCEDURE AND SETUP

Rings of commercial Fe-Co-V sheets (Vacoflux®, thickness $d = 0.201$ mm; Vacodur®, $d = 0.10$ mm) were subjected, after cutting, to standard annealing treatment in vacuum (10 hours at 820 °C), followed by ~ 100 °Cs^{-1} cooling, down to $T \sim 300$ °C. The same treatment was applied to Vacoflux Epstein strips. Five Vacoflux rings (prepared at INRIM) were stacked to form toroidal samples of outside diameter $D_o = 100$ mm and inside diameter $D_i = 80$ mm. The Vacodur toroid (prepared at NPL) was made of 70 stacked rings ($D_o = 38.04$ mm, $D_i = 31.62$ mm). It was jointly tested in the two cooperating laboratories. The magnetic path length was taken for the two samples as $l_m = \pi\ (D_o - D_i)/\ln(D_o/D_i)$. A few physical parameters of the investigated alloys are listed in Table 1. The magnetic measurements were performed between 2 Hz and 5 kHz by means of a calibrated hysteresisgraph-wattmeter, with peak polarization value J_p ranging between 1.0 T and 1.9 T. Sinusoidal secondary voltage was maintained, under all circumstances, by digital feedback. The measurement principles and the general features of the employed setup, which works in a 12-bit signal acquisition environment, are discussed in [10]. The measurements were made between 2 Hz and 5 kHz at temperatures T ranging between −50 °C and 155 °C. To this end, the measuring sample was placed in a climate chamber (in air), where the required temperature was reached and stabilized. The upper T value corresponds to the maximum operating temperature of the "F class" insulation, (IEC 60085, IEC 60034-1), matching typical operating temperatures of electric motors, and extending the current 23 ± 5 °C temperature requirements of IEC 60404 standards. The normal DC curves were also measured at room temperature by the ballistic method (IEC 60404-4), while the quasi-static energy loss W_{hyst} was obtained and separated from the dynamic loss $W_{dyn}(f)$ by extrapolating the measured $W(f)$ curves to the limit $f \to 0$, according to a precise scheme, connected with the loss decomposition procedure [11].

TABLE 1. Physical parameters of the Fe-Co sheets.

Material	Thickness d (mm)	Density δ(kg/m^3)	Conductivity σ at 23 °C (Ω^{-1}m^{-1})	Conductivity σ at 155 °C (Ω^{-1}m^{-1})	Thermal expansion coefficient (K^{-1})
Vacoflux	0.201	8120	$2.32 \cdot 10^6$	$2.10 \cdot 10^6$	$9.5 \cdot 10^{-6}$
Vacodur	0.10	8120	$2.35 \cdot 10^6$	$2.12 \cdot 10^6$	$9.5 \cdot 10^{-6}$

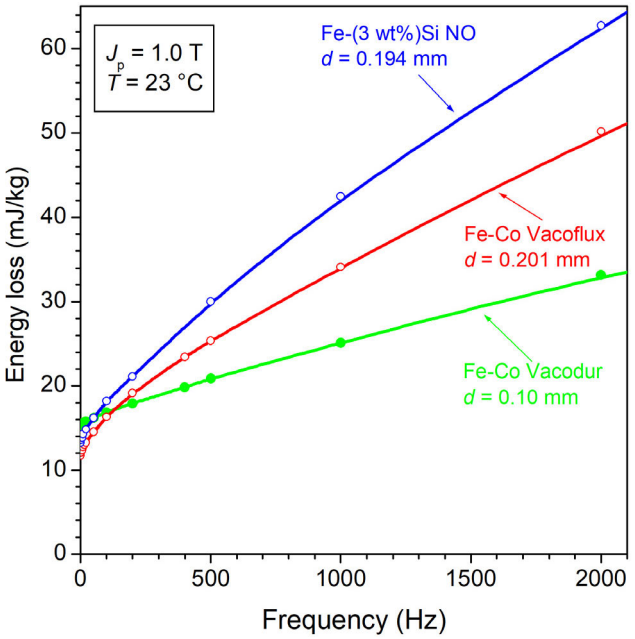

FIGURE 1. Energy loss W(f) versus frequency measured up to 2 kHz at peak polarization value $J_p = 1.0$ T in thin soft magnetic sheets: 1) NO Fe-(3wt%)Si ($d = 0.194$ mm), (RD + TD) Epstein strips (IEC 60404-10); 2) Fe-Co Vacoflux ($d = 0.201$ mm) ring sample; 3) Fe-Co Vacodur ($d = 0.1$ mm) ring sample.

A general overview of the energy loss dependence on frequency and temperature is provided in Figs. 1 and 2. We see in Fig. 1 that the 0.10 mm thick Vacodur sheets exhibit the highest W_{hyst} and the lowest dynamic loss $W_{dyn} = W_{class} + W_{exc}$(at least beyond few hundred Hz). It is noted how the 0.194 mm Fe-(3 wt%)Si sample displays everywhere the highest W_{dyn}, in spite of higher resistivity than Fe-Co ($52{\cdot}10^{-8}$ Ωm vs. $43{\cdot}10^{-8}$ Ωm). It is noted that these Fe-Si sheets are endowed with a large grain size ($< s > = 122\ \mu$m), a property conducive to a large contribution by the excess loss [9]. Fig. 2 provides an example of passage of $W(f)$ through a minimum value around 23 °C in the Fe-Co alloys, in contrast with the monotonical decrease observed in Fe-Si. This property of Fe-Si is easily justified in terms of anisotropy energy constant K and conductivity σ concurrently decreasing with T. Additional effects are responsible for the more complex response of Fe-Co, as clarified in the following via the loss decomposition procedure.

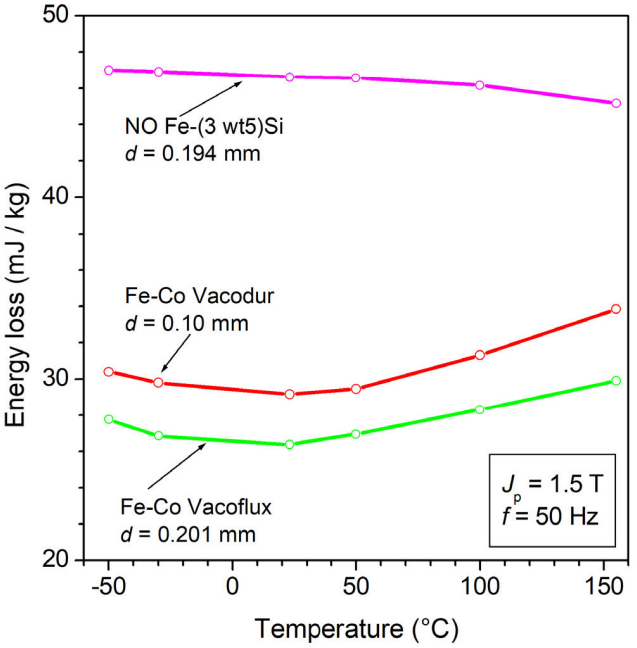

FIGURE 2. The energy loss W(f) measured in the Fe-Co Vacoflux sample at $J_p = 1.5$ T exhibits a passage through a minimum value around $T = 23$ °C at 50, 200, and 400 Hz. The same trend is observed in the Fe-Co Vacodur sheets, in contrast with the monotonical decrease of W(f) exhibited by the NO Fe-Si alloy.

III. RESULTS AND DISCUSSION

A. LOSS DECOMPOSITION: THE CLASSICAL EDDY CURRENT LOSS

The less-than-linear increase of $W(f)$ with frequency, the landmark feature of the magnetic losses in steel sheets, is well illustrated by the results shown in Fig. 1. Non-linearity is entirely due, as long as the skin effect is not involved, to the excess loss contribution, which is generally described, in theory and experiment, according to Bertotti's model, which predicts an $f^{1/2}$ dependence [12]. In the present broadband investigation, however, the skin effect plays a role and, although the physical concept of loss decomposition is still appropriate, an approach aiming at the determination of the loss components under non-uniform flux profile across the sample sheet has been developed. It appears, that the expression for the classical eddy current loss at peak polarization value J_p, as provided by the Maxwell's diffusion equation, in the absence of dielectric effects, for full flux penetration in a sheet of thickness d, conductivity σ and mass density δ

$$W_{class}\left(J_p, f\right) = \frac{\pi^2}{6\delta} \cdot \sigma J_p^2 d^2 f, \quad [\text{J/kg}] \tag{1}$$

does not hold beyond a few hundred Hz in the 0.20 mm thick Vacoflux sheet. It is still acceptable up to about 1 kHz in the 0.1 mm thick Vacodur samples, taking advantage of lower thickness and permeability.

The comprehensive calculation of $W_{class}(f)$ in soft magnetic laminations, inclusive of the skin effect, requires a sophisticated approach to the electromagnetic diffusion equation in a medium locally described by a hysteretic constitutive relationship [13], [14]. It is generally implemented by means of a quasi-static hysteresis model (e.g., the Preisach hysteresis model) and a sound numerical procedure, ensuring convergence [15], [16]. This involves, however, a large computational burden, which can be partly overcome, at the cost of a certain approximation, by adopting the normal magnetization curve $B(H)$ as the constitutive magnetic equation of the material [17]. For an infinitely extended lamination in the y-z plane parallel to its surface and an alternating field applied in this plane (e.g., in the -z direction) a scalar relationship between local field $H(x)$ and induction $B(x)$, exclusively depending on the coordinate x normal to the sheet plane ($-d/2 \le x \le d/2$), can be defined. The half thickness of the sheet is subdivided into an adequately large number of layers and to each of them the Maxwell's diffusion equation applies

$$\partial^2 H\,(x)\,/\partial x^2 = \sigma\,\partial B(x)/\partial t, \tag{2}$$

For rated induction value $\overline{B}(t)$, average of $B(x, t)$ across the sheet thickness, the problem is solved by introducing the vector potential $A(x, t)$ and its relationship to the induction $B(x, t) = \nabla \times A(x, t)$. Because of the symmetry of the problem,

$$B(x) = -\partial A(x)/\partial x \tag{3}$$

and the diffusion equation becomes

$$\partial H(x)/\partial x + \sigma\,\partial A\,(x)\,/\partial t = 0. \tag{4}$$

One way of solving (4) for non-linear $B(H)$ relationship is by application of the fixed-point method [18], [19], where the non-linear operator H is linearized according to the equation

$$H\,(x, t) = \nu_{FP} B\,(x, t) + R\,(x, t)\,. \tag{5}$$

The reluctivity ν_{FP} in (5) is assumed constant and R is a residual term, to be determined by iterative calculation of (4), expressed as

$$\nu_{FP}\partial^2 A/\partial x^2 - \sigma\,\partial A/\partial t = \partial R/\partial x, \tag{6}$$

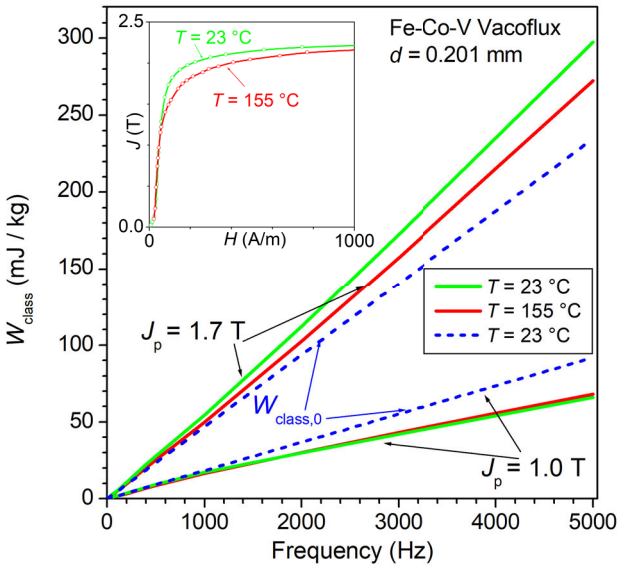

FIGURE 3. The classical energy loss component $W_{class}(f)$ is calculated in the Vacoflux sheet at 23 °C and 155 °C up to f = 5 kHz taking into account the skin effect (8). The dashed lines ($W_{class,0}$), linearly increasing with f, are calculated by (1), disregarding the skin effect. To note the opposite deviations from linearity brought about by the skin effect at low and high J_p values. Inset: normal magnetization curves measured at 23 °C and 155 °C.

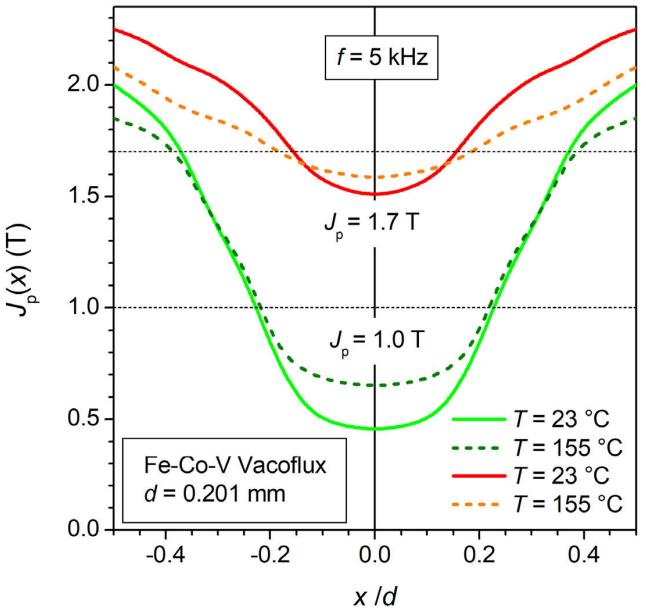

FIGURE 4. Profiles of the local peak polarization values $J_p(x/d)$ across the sheet thickness d calculated at the frequency f = 5 kHz by the recursive application of the Maxwell's diffusion equation. The shown profiles are obtained for the measured peak polarization values J_p = 1.0 T and 1.7 T. These profiles pair with the behaviors of $W_{class}(f)$ shown in Fig. 3. To note that the concept of skin depth does not apply under these circumstances.

with the boundary conditions

$$A(0,t) = 0; A(\pm d/2, t) = -\overline{B(t)}(t) \cdot d/2. \quad (7)$$

The ν_{FP} value is appropriately chosen on the $B(H)$ curve for best convergence and $R(x,t)$ is updated by successive iterations, starting from a trial value (typically zero). Under periodic excitation, the problem is best treated, as discussed in detail in [13] and [18], by expressing (6) in the Fourier domain, using a conveniently high number N of harmonics (for example 20) and solving the involved sequence of N linear equations. The lamination is subdivided into a suitable number of layers (typically 40 in these calculations) and the diffusion equation is solved in each layer for each harmonic, going then back, at each iteration step, to a time dependent solution $A(x, t)$ by inverse Fourier transform. The process is iterated till $R(x,t)$ is stabilized, according to (5). The induction $B(x, t)$ is then obtained by (3). W_{class} is finally calculated by integrating the product of the field at the lamination surface (i.e., the applied field) $H(d/2, t)$ with $d\overline{B(t)}/dt$

$$W_{class}(f) = \frac{1}{\delta}\int_0^{1/f} H(d/2,t)\cdot(d\overline{B}/dt)dt \quad [J/kg] \quad (8)$$

Fig. 3 provides an example of $W_{class}(f)$ calculated in the 0.201 mm thick Vacoflux sheet up to 5 kHz. The deviation from the linear increase with f predicted by (1) ($W_{class,0}$) is apparent, as well as the different diverging trends observed for $J_p = 1.0$ T and $J_p = 1.7$ T. This is understood by looking at the profiles $J_p(x)$ of the maximum polarization values, as obtained by the recursive calculations, at different depths across the lamination thickness (Fig. 4). With the sheet core partially depleted of magnetization reversal ($J_p(x) < J_p$) and the long-range eddy current patterns crowded towards the sheet surface, $W_{class}(f)$ is decreased with respect to the case of homogeneous flux. This is what is shown for $J_p = 1.0$ T in Figs. 3 and 4. However, the $J_p(x)$ profile evolves, because of incipient saturation at the sheet surface, under increasing J_p. For example, progressive narrowing and smoothing of the $J_p(x) < J_p$ well at the sheet core is predicted in Fig. 4 for $J_p = 1.7$ T and $f = 5$ kHz. This engenders an opposite effect on $W_{class}(f)$, as observed in Fig. 3. To remark that such profiles, influenced by non-linearity of $J(H)$ and the eventual approach to magnetic saturation, hide the underlaying phase relationships among the $J_p(x, t)$ waveforms at different depths x. One cannot properly talk of skin depth under such circumstances. It is also clear in Fig. 4 how the increase of resistivity with temperature (from $43{\cdot}10^{-8}$ Ωm to $48{\cdot}10^{-8}$ Ωm on passing from 23 °C to 155 °C), combined with the observed variation of the normal magnetization curve, leads to smoothing of the $J_p(x)$ profiles, with obvious effects on the $W_{class}(f)$ curves.

B. LOSS DECOMPOSITION: HYSTERESIS AND EXCESS LOSSES

Once the broadband calculation of $W_{class}(f)$ is carried out at different J_p values and different temperatures, the full loss decomposition can be achieved. We extrapolate first the quantity $W(f)$ - $W_{class}(f)$ to $f = 0$ and we obtain the hysteresis loss component W_{hyst} in the absence of skin effect. W_{hyst} is in fact independent of frequency [12], up to the point where, like in the example shown in Fig. 4, the appearance of a strongly

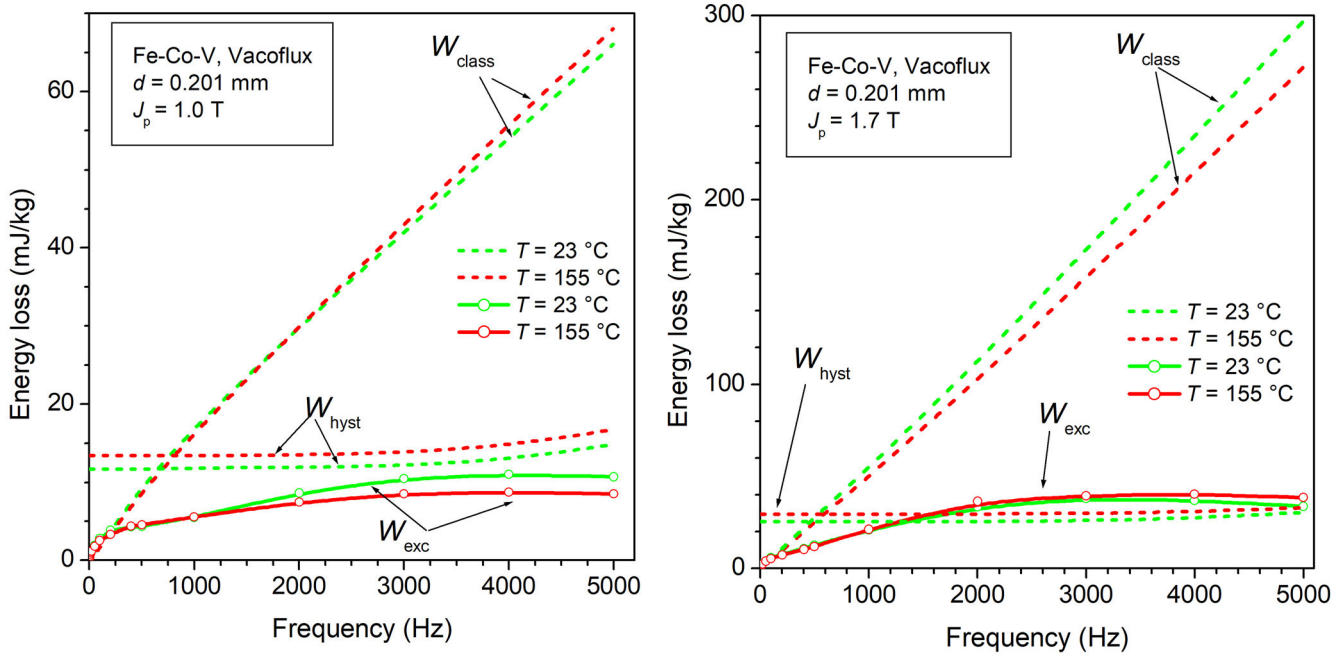

FIGURE 5. Energy loss decomposition in the 0.201 mm thick Vacoflux samples up to 5 kHz. Two J_p values at 23 °C and 155 °C are considered. The classical loss W_{class} is calculated first with (8), which coincides with (1) below about 1 kHz. W_{hyst} at low frequencies is thereby obtained by the usual extrapolation procedure of W(f) - W_{class}(f) to f → 0. W_{hyst} starts to increase with f, according to the calculated profile $J_p(x)$ and (9), upon attaining the kHz range. The excess loss W_{exc}(f) tends to flatten at the same time. The high-frequency contribution by W_{hyst} and W_{exc} to W(f), reflecting the dissipation by the eddy currents localized at and about the moving domain walls, is overwhelmed by W_{class} when J_p is around and beyond the knee of the magnetization curve (see inset in Fig.3).

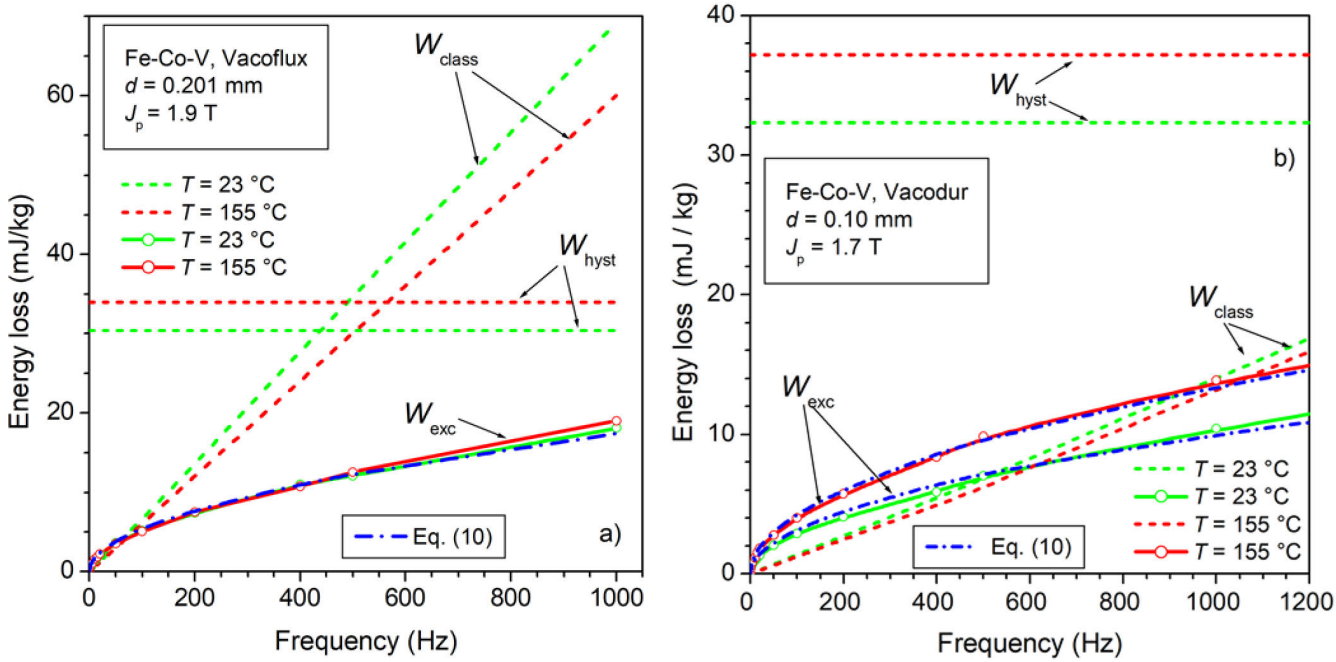

FIGURE 6. a) Energy loss decomposition in the 0.201 mm thick Vacoflux up to 1 kHz for $J_p = 1.9$ T. The skin effect is barely recognized in this frequency range and $W_{class}(f)$ can be calculated with either (1) or (8). W_{hyst} is thus nearly independent of f, whereas $W_{exc}(f)$ follows to good extent the usual $f^{0.5}$ law and can be well predicted by (10) (dash-dotted line). b) Same as (a) in the 0.10 mm thick Vacodur sample.

non-uniform $J_p(x)$ profile is conducive, because of the more than linear W_{hyst} dependence on J_p, to an increase of W_{hyst} with f (J_p is obviously assumed here to be the thickness-averaged $J_p(x)$). The hysteresis loss has a local character, because it is associated with the elementary Barkhausen jumps, and is expected to evolve from the sheet midplane to the surface according to the $J_p(x)$ profile. The power law $W_{hyst} = k\, J_p^n$, with n = 1.45 and k a proportionality constant,

applies in the present case and we calculate at any frequency

$$W_{\text{hyst}}\left(J_{\text{p}},f\right)=\frac{1}{d}\int_{-\frac{d}{2}}^{\frac{d}{2}}k(J_{\text{p}}\,(x))^{\text{n}}dx. \tag{9}$$

We arrive at the broadband energy loss decomposition illustrated in Fig. 5, where W_{hyst}, W_{class}, and W_{exc} calculated in the Vacoflux sheet are shown for $J_{\text{p}} = 1.0$ T and 1.7 T up to 5 kHz. On entering the kHz range, W_{hyst} starts to moderately increase, whereas $W_{\text{exc}}(f)$ slows down its dependence on f. The more than linear $W_{\text{hyst}} = k\,J_{\text{p}}^{\text{n}}$ relationship justifies, via (9), the increase of $W_{\text{hyst}}(f)$ with the deepening of the skin effect. On the other hand, $W_{\text{exc}}(f)$, deriving from eddy current patterns circulating at the domain scale, appears to attain a behavior intermediate between $W_{\text{hyst}}(f)$ and $W_{\text{class}}(f)$. Its formulation in the presence of the skin effect would require, as discussed in [17], adaptation of the expression provided by the Statistical Theory of Losses (STL)

$$W_{\text{exc}}\left(J_{\text{p}},f\right)=(\frac{8.76}{\delta})\sqrt{\sigma GSV_0 f}J_{\text{p}}^{3/2},\quad [\text{J/kg}] \tag{10}$$

where $G = 0.1356$, S is the sample cross-sectional area, and V_0 is a statistical parameter, expressed in Am^{-1}. We observe in Fig. 6 that (10) fits the experimental $W_{\text{exc}}(f)$ up to about 1 kHz, but it is fair to say that the statistics of the local magnetization reversals, as well as the domain structure, may unpredictably evolve under deep skin effect. The previous classical calculation in Fig. 4 shows that $J_{\text{p}}(x)$ attains values not far from the saturation value J_{s} on approaching the sheet surface ($x = \pm\, d/2$, Fig. 4). This finding consistently compares with the behavior of the experimental hysteresis loops in Fig. 7, where we observe that the strength of the applied field (i.e. the effective field at the sheet surface) at high frequencies (5 kHz in this example) is the one required, according to the experimental magnetization curves shown in Fig. 3, for securing such high polarization values. We thereby conclude that the magnetization process at and close to the sheet surface partly and increasingly occurs, depending on J_{p}, by rotations under increasing frequencies. In fact, the rotation associated loss lumps into $W_{\text{class}}(f)$, resulting in the waning increase of $W_{\text{exc}}(f)$ with f put in evidence in Fig. 5.

C. THE EFFECT OF TEMPERATURE

1) THE HYSTERESIS LOSS

We have anticipated in Fig. 2 the somewhat abnormal dependence of the 50 Hz energy loss on temperature exhibited by the Fe-Co-V alloys Vacoflux and Vacodur in the range $-50\ ^{\circ}\text{C} \le T \le 155\ ^{\circ}\text{C}$. $W(f)$ is observed to pass through a shallow minimum around room temperature. This contrasts with the typical monotonical decrease of $W(f)$ with T occurring in most crystalline magnetic materials, as illustrated for a NO Fe-(3 wt%)Si alloy in Fig. 2. These properties are repeatably verified in all the investigated temperature range, irrespective of the specific thermal cycle imposed by the measurements. The material is in a stable structural state, and no ancillary order-disorder transformations occur in the samples. To improve our physical insight in these behaviors, we exploit

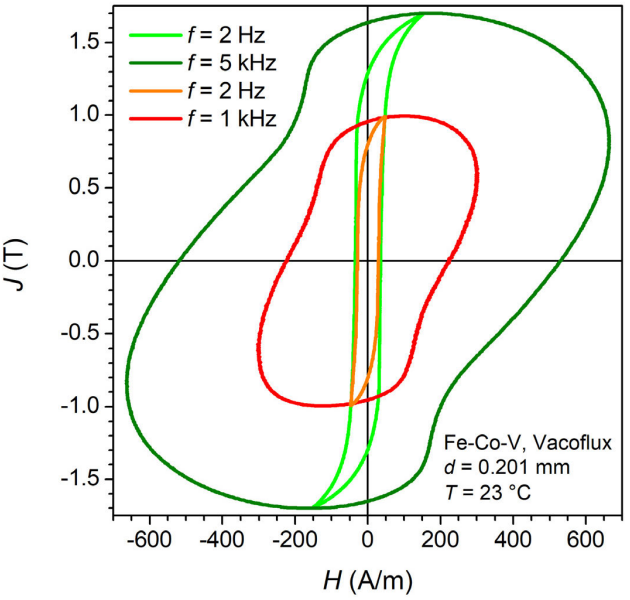

FIGURE 7. Hysteresis loops in the Vacoflux sheet measured under quasi-static excitation and at $f = 5$ kHz. The applied field, coincident with the effective field at the sheet surface, attains at 5 kHz values compatible with the predicted $J_{\text{p}}(d/2)$ in Fig. 4. In fact, $J_{\text{p}}(x)$ becomes close to saturation on approaching $x = \pm d/2$, as put in evidence by the normal magnetization curves in Fig. 3.

the loss decomposition and we separate the quasi-static from the dynamic loss properties. We then observe how the quasi-static loss $W_{\text{hyst}}(J_{\text{p}})$ and the associated hysteresis loops evolve with T in Figs. 8 and 9. It is natural to attribute the minimum of the $W_{\text{h}}(J_{\text{p}})$ versus T dependence to contrasting temperature-dependent material properties, which affect the magnetization process. We identify such properties in the magnetocrystalline and magnetostrictive energies. It is well recognized that, following a treatment leading to a partially ordered state, the anisotropy constant K_1 of Fe-Co-V can reach quite low values, of the order of few hundred J/m^3, conducive in principle to very soft magnetic properties [20], [21], [22]. At the same time, the magnetostriction constant, little dependent on the state of order and temperature, attains values as high as $\lambda_{\text{s}} \sim 70{\cdot}10^{-6}$ [22], [23], [24]. Because of these unique circumstances, any state of applied or residual stress can appreciably influence the soft magnetic response of the alloy. We state that the internal stresses arising under any change of temperature magnetostrictively interfere with the magnetization process. They compound with the effect of the anisotropy energy K_1 and its temperature dependence, to give rise to the observed evolution of hysteresis loop and loss with T. Let us then consider a state of the material, where ordered α' regions are embedded in a disordered α matrix. Coexistence of ordered and disordered regions, having different lattice parameters and different thermal expansion coefficient γ [24], gives rise, at all temperatures, to a state of random internal stresses, with wavelength defined by size and distribution of the α and α' regions in the material. Compressive and tensile stresses operate in a different manner on the population of easy axes occupied by the main domains, either

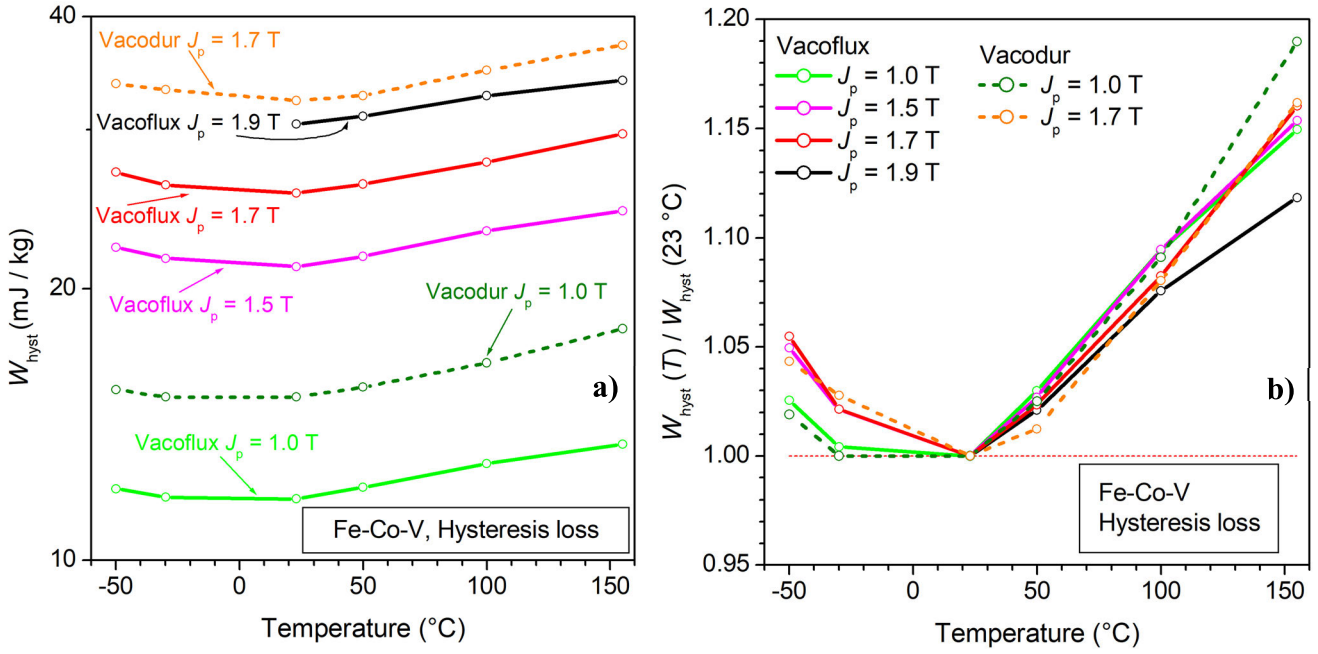

FIGURE 8. Hysteresis (DC) loss component W_{hyst} and its temperature dependence in Vacoflux and Vacodur sheets for J_p ranging between 1.0 T and 1.9 T. The same quantities, normalized to their values at $T = 23$ ° C, are shown in (b) .

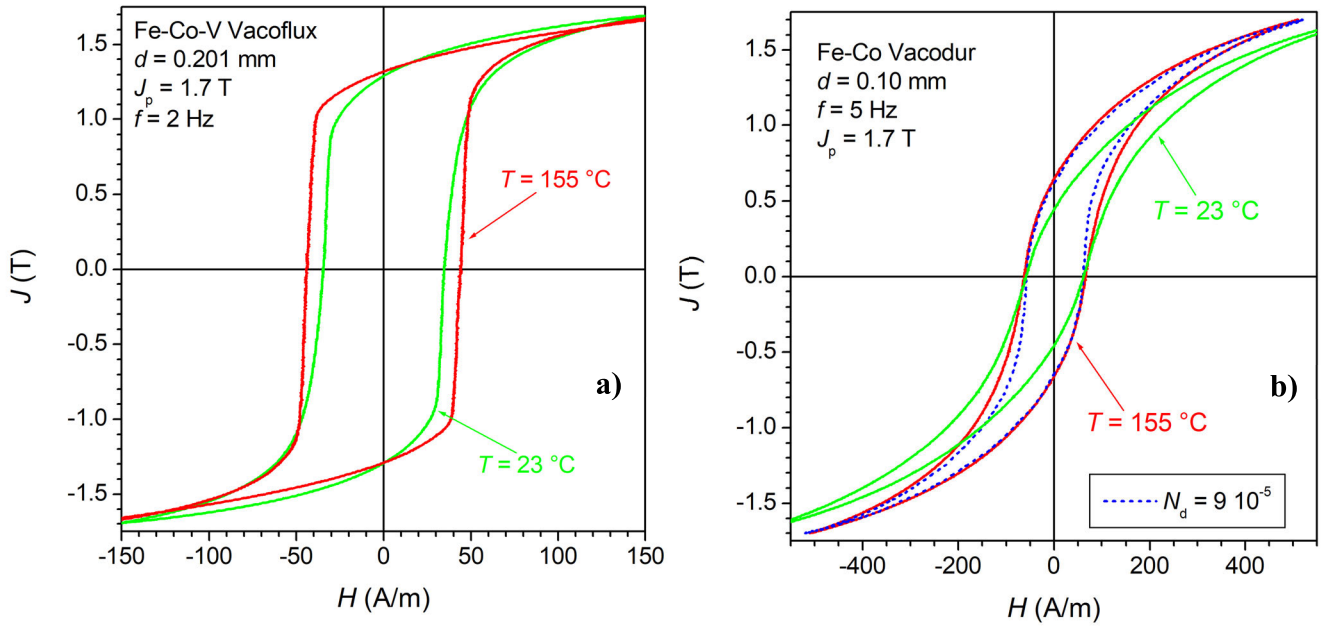

FIGURE 9. Quasi-static hysteresis loops at $J_p = 1.7$ T measured at 23 °C and 155 °C in the Vacoflux (a) and Vacodur (b) sheets. The increase of temperature brings about sharpening of the loop and increase of its area. To note how the role of the internal demagnetizing field is brought to light on passing from from 23 °C to 155 °C in the Vacodur sample. It decreases under increasing T, as shown by the behavior of the loop taken at 23 °C after reconstruction via a suitable demagnetizing factor N_d (dashed line in (b)).

favoring (tension) or disfavoring (compression) the axes lying closer to the stress direction. Any change of temperature modifies the stress pattern and engenders a definite local magnetostrictive energy change E_λ, which combines with the local anisotropy energy E_K, entering both the domain wall energy and the domain pattern. To make an order of magnitude estimate of E_λ, we take such a difference to be as small as $\Delta\gamma \sim 2.5{\cdot}10^{-7}$ K^{-1} [24], versus a declared thermal expansion coefficient of the alloy $\gamma = 9.5{\cdot}10^{-6}$ K^{-1} [25]. For a temperature change ΔT, we estimate a variation of the local internal stress, ensuing from the different dilatometric response of ordered and disordered phases, $\Delta\sigma\Delta s = \Delta\gamma \cdot \Delta T \cdot Y(T)$, where the Young modulus at room temperature is $Y = 200$ GPa [25]. $Y(T)$ decreases by a few percent on going from room temperature to $T = 150$ °C, while $\Delta\gamma$ is quite independent of T [26]. $\Delta\sigma\Delta s \sim 5$ MPa for $\Delta T =$

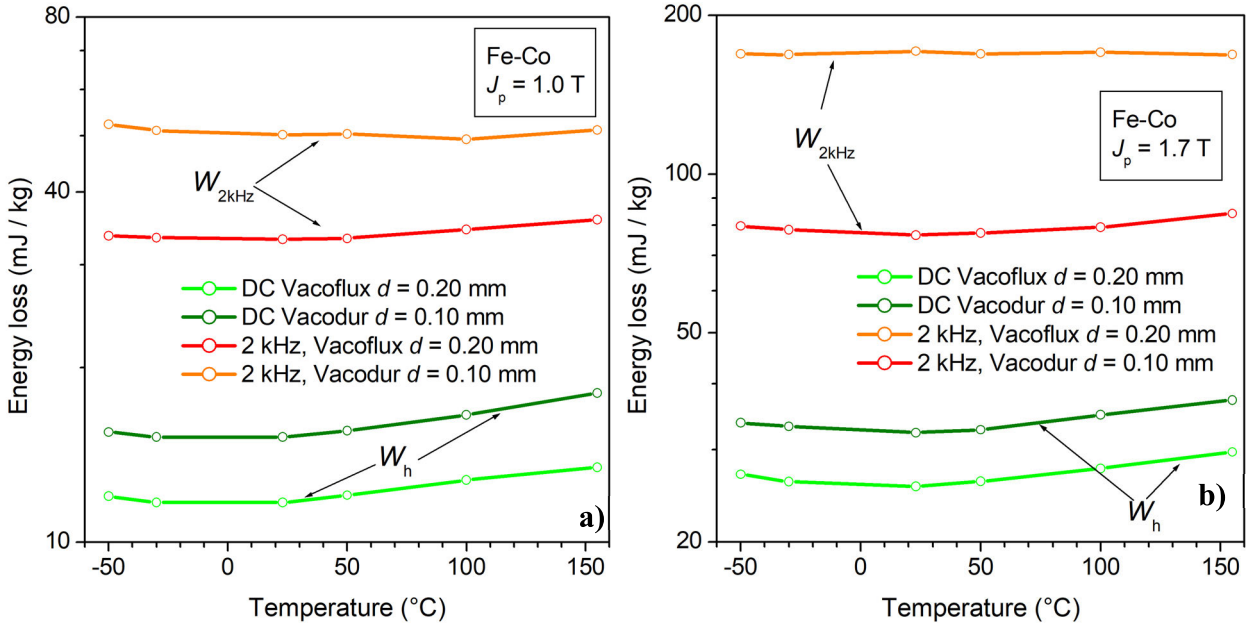

FIGURE 10. Temperature dependence of the quasi-static energy loss W_{hyst} and the loss W(f) measured at 2 kHz in the Vacoflux and Vacodur sheets at $J_p = 1.0$ (a) and $J_p = 1.7$ T (b). At high frequencies ($f > 2$ kHz), the dynamic loss in the thicker Vacoflux sample largely compensates for the dependence of W_{hyst} on T (see Fig. 5) and W(f) starts to decline monotonically with T, following the behavior of W_{class}.

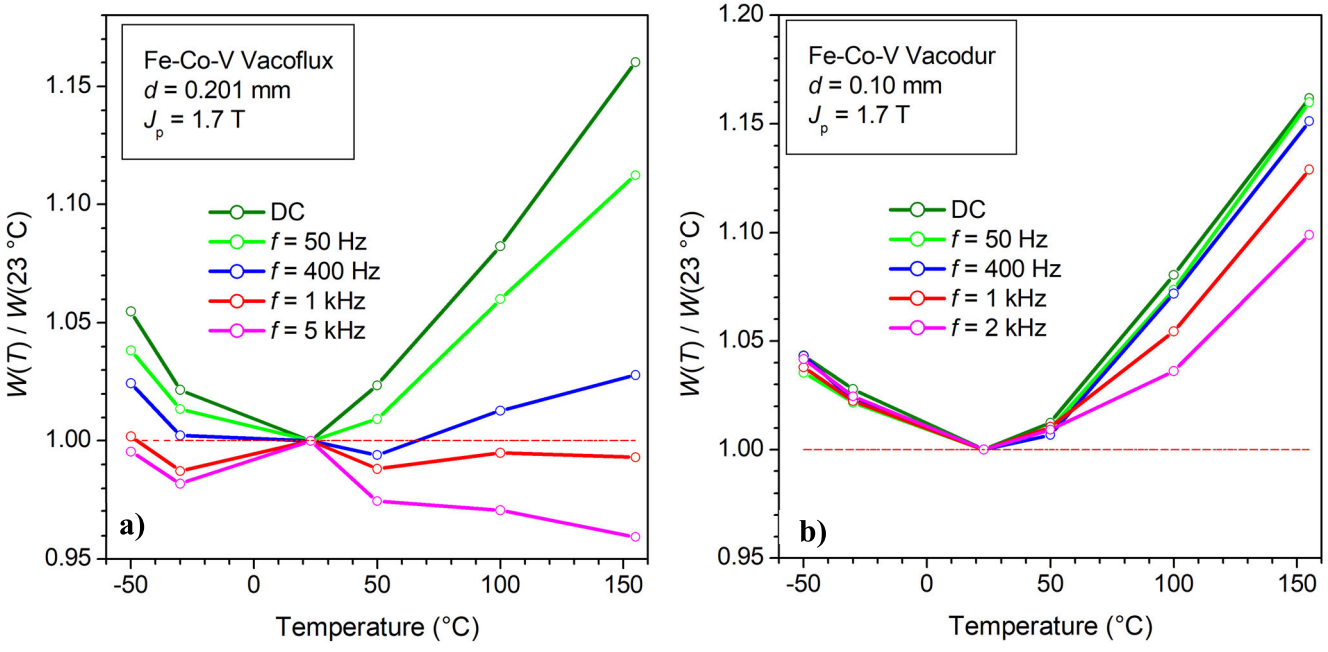

FIGURE 11. Energy loss W(f) , measured up to $f = 5$ kHz, normalized for each selected frequency to the value taken at $T = 23$ °C. W(f) tends to progressively loosen its dependence on T under increasing frequencies, because of the increase of the dynamic loss components. With a prominent role played by $W_{class}(f)$ beyond about 1 kHz (see Fig. 5), W(f) eventually tends to monotonically decrease with T in the thicker Vacoflux sample, following the increase of the resistivity.

100 °C can therefore be envisaged and the corresponding magnetostrictive energy density variation, averaged over all possible orientations of the easy axes, calculated as $E_\lambda = \lambda_s \Delta\sigma \Delta s \sim 350$ J/m^3. The increasing trend of W_{hyst} versus T points then to an associated increase of the internal stress. We conclude that E_λ and K_1 can have comparable, but opposite trends with T. In fact, K_1 decreases with increasing T, as is usually the case and is possibly verified by comparing the quasi-static hysteresis loops obtained at 23 °C and 155 °C in Epstein strips cut along the rolling direction (RD) and the transverse direction (TD). The slight anisotropic advantage of the RD Vacoflux sheets, lumped in the parameter $R_{hyst} = (W_{hyst,RD}(1.7\ T) / W_{hyst,TD}(1.7\ T)) = 0.95$ observed at 23 °C, nearly disappears at 155 °C, where $R_{hyst} = 0.99$, pointing to the concurrent decrease of K_1. The increase of W_{hyst} with T will therefore derive from the increase of the

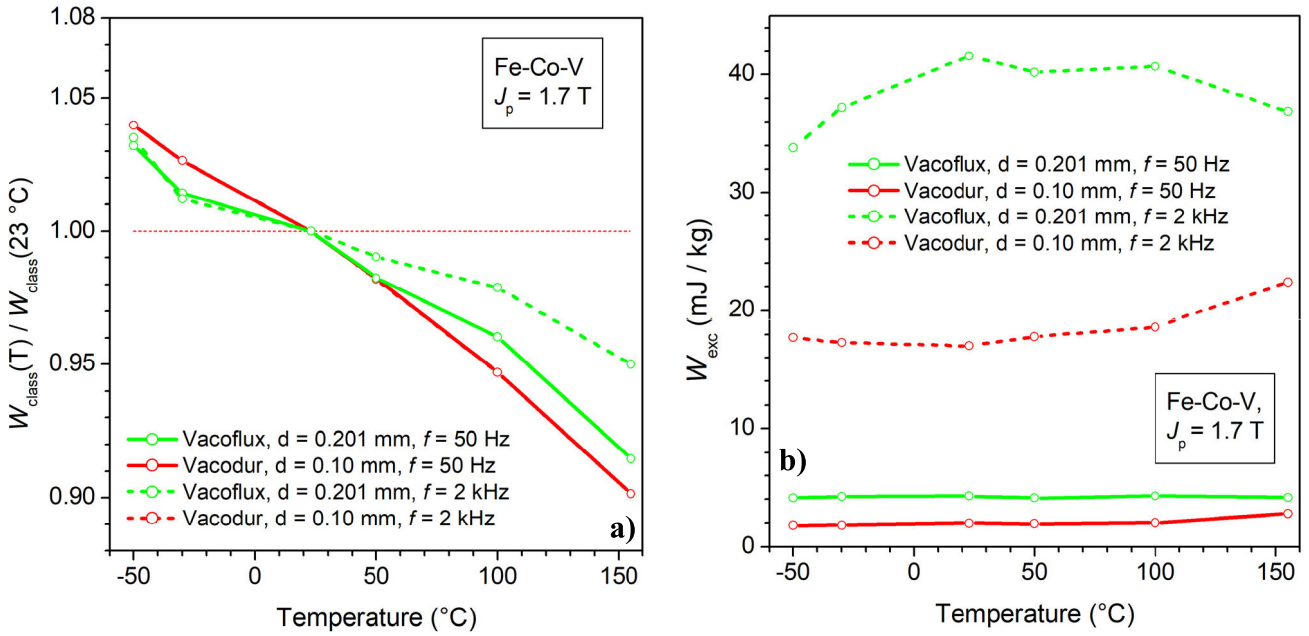

FIGURE 12. a) Classical loss $W_{class}(f)$, normalized to the value at $T = 23$ °C, calculated at 50 Hz and 2 kHz as a function of temperature in the Vacoflux and Vacodur sheets. Peak polarization value $J_p = 1.7$ T. b) Correspondingly obtained excess loss $W_{exc}(f)$. The skin effect plays a role in the loss decomposition at 2 kHz in the Vacoflux sheets, while weakly affecting the loss in the thinner Vacodur samples.

thermally induced stresses and the ensuing magnetostrictive evolution of domain structure, domain wall pinning, and internal demagnetizing fields. The shape of the hysteresis loops in Fig. 9 denotes a decrease of the internal demagnetizing effects, related more to changing flux closure at the boundaries between ordered and disordered regions (having different J_s values [24]) than to the decrease of J_s with T. This would justify the simultaneous increase of coercive field and differential permeability by a mechanism of inhibition of the germs for nucleation of reverse domains during remagnetization. This effect is especially prominent in the Vacodur sheets. It is observed in Fig. 9b how a great deal of the hysteresis loop measured at 155 °C is retrieved by correcting the loop taken at 23 °C using the demagnetizing factor $N_d = 9{\cdot}10^{-5}$.

2) THE DYNAMIC LOSS

The previously shown loss separation curves are instrumental in the search for a rationale in the $W(f)$ dependence on temperature. We have already emphasized that the minimum value attained by $W(f)$ about the room temperature appears to coherently descend from the behavior of $W_{hyst}(T)$ (Figs. 8 and 9). Regarding the dynamic loss, we realize first, looking at Figs. 10 and 11, that the dependence of $W(f)$ with T is smoothed out with increasing frequency, eventually attaining a nearly monotonic decrease with T in the thicker Vacoflux sheet beyond $f = 1$ kHz. As f is increased, the contribution by W_{hyst} is progressively obscured by the increase of $W_{dyn}(f) = W_{class}(f) + W_{exc}(f)$. Figs. 5 and 6 make clear that $W_{class}(f)$, becoming dominant with respect to W_{hyst} and $W_{exc}(f)$, chiefly contributes to such a behavior. The $W(f)$ dependence on T will eventually identify with the dependence of $W_{class}(T)$. Figs. 10 and 11 show that this phenomenology is delayed, for a same J_p value, to higher frequencies in the thinner Vacodur sheets. Fig. 12a shows that $W_{class}(f)$ follows a monotonical decrease with T at low (50 Hz) and high (2 kHz) frequencies, as predicted by (1) via the conductivity decrease with T (Table 1), in the 0.10 mm thick Vacodur sheets and by taking into account the skin effect at 2 kHz (Eq. (8)) in the 0.201 mm thick Vacodur samples. The relative proportions of $W_{class}(f)$ with respect to $W(f)$ and the other components can be appreciated in Figs. 5 and 6. Fig. 6b shows that W_{exc} and W_{hyst} follow a same trend with T. The STL predicts that such a connection is plausible, as it descends from the relationship existing between the parameter V_0 in (10) and the coercive field [12]. W_{exc} exhibits, for same J_p and f, quite higher values in the Vacoflux sheets and a somewhat opposite trend versus T (see Fig. 12b). This points, on the one hand, to a more discrete nature of the magnetization process in Vacoflux, which is the conclusion we get when comparing the shapes of the quasi-static hysteresis loops in the two materials (Fig. 9). On the other hand, the dependence of W_{exc} on T at high frequencies is made complex by the skin effect and the partial establishment of rotations in the regions further from the sheet core, which interfere with the statistics of the domain wall processes.

IV. CONCLUSION

Commercial Fe-Co-V alloys can exhibit remarkable loss advantage with respect to high-grade non-oriented Fe-(3 wt%)Si sheets of comparable thickness. However, its energy loss figure is observed to increase, across a wide frequency range, upon increasing the temperature T beyond room temperature. This contrasts with the decrease of the loss usually

observed in the Fe-Si alloys and in most soft magnetic materials. By loss decomposition and identification of hysteresis W_{hyst}, classical W_{class}, and excess W_{exc} losses, we obtain that this effect is chiefly associated with the dependence of W_{hyst} with T. The assumed mechanism by which W_{hyst} increases with T is the generation of local stresses following the different thermal expansion of the superlattice regions α' and the disordered matrix α. The correspondingly created energy E_λ in these highly magnetostrictive materials can amount to a few J/m^3 per degree centigrade, thereby competing with the decrease with temperature of the magnetocrystalline energy E_{K}, whose value at room temperature can be of the order of a few hundred J/m^3. It turns then out that a minimum value for $E_\lambda + E_{\text{K}}$ can engender, around room temperature, a minimum of coercivity and quasi-static loss. With increasing the magnetizing frequency, different roles are played by W_{class}, and W_{exc}, which are not easily quantified in the kHz range, because of the skin effect. Phenomenologically, progressive leveling of the $W(f)$ dependence on T occurs, eventually evolving into a monotonic decrease with T beyond about 2 kHz in the Vacoflux sheets. At such frequencies, the non-homogeneous flux profile across the sheet thickness must be taken into account. This is calculated by solving the Maxwell's diffusion equation with a numerical procedure, where the magnetic constitutive equation of the material is identified with the normal (initial) $B(H)$ quasi-static curve. In this way, the loss decomposition versus frequency is done up to 5 kHz, bringing to light a decreasing contribution by W_{exc} with respect to W_{class}, thereby inducing a transition towards monotonical decrease with T of the loss at high frequencies.

REFERENCES

[1] R. S. Sundar and S. C. Deevi, "Soft magnetic FeCo alloys: Alloy development, processing, and properties," *Int. Mater. Rev.*, vol. 50, no. 3, pp. 157–192, Jun. 2005, doi: 10.1179/174328005X14339.

[2] T. Waeckerlé, R. Batonnet, T. Wéry, and F. Petit, "Fully processed Fe-Co soft magnetic laminations for high-speed electrical machines," *IEEE Trans. Magn.*, vol. 50, no. 4, pp. 1–6, Apr. 2014, doi: 10.1109/TMAG.2013.2286629.

[3] R. Pandey, M. Weichold, and D. Palmer, "Materials characterization for high temperature transformers," *IEEE Trans. Magn.*, vol. MAG-16, no. 5, pp. 749–751, Sep. 1980, doi: 10.1109/TMAG.1980.1060741.

[4] R. T. Fingers, R. P. Carr, and Z. Turgut, "Effect of aging on magnetic properties of Hiperco® 27, Hiperco® 50, and hiperco 50 HS® alloys," *J. Appl. Phys.*, vol. 91, no. 10, pp. 7848–7850, May 2002, doi: 10.1063/1.1453939.

[5] R. H. Yu, S. Basu, L. Ren, Y. Zhang, A. Parvizi-Majidi, K. M. Unruh, and J. Q. Xiao, "High temperature soft magnetic materials: FeCo alloys and composites," *IEEE Trans. Magn.*, vol. 36, no. 5, pp. 3388–3393, 2000, doi: 10.1109/20.908809.

[6] R. H. Yu and J. Zhu, "Precipitation and high temperature magnetic properties of FeCo-based alloys," *J. Appl. Phys.*, vol. 97, no. 5, Mar. 2005, Art. no. 053905, doi: 10.1063/1.1857057.

[7] W. Pieper and J. Gerster, "Total power loss density in a soft magnetic 49% Co–49% Fe–2% V-alloy," *J. Appl. Phys.*, vol. 109, no. 7, Apr. 2011, doi: 10.1063/1.3537956.

[8] C. Beatrice, C. Appino, O. de la Barrière, F. Fiorillo, and C. Ragusa, "Broadband magnetic losses in Fe-Si and Fe-Co laminations," *IEEE Trans. Magn.*, vol. 50, no. 4, pp. 1–4, Apr. 2014, doi: 10.1109/TMAG.2013.2286923.

[9] N. Leuning, S. Steentjes, and K. Hameyer, "Effect of grain size and magnetic texture on iron-loss components in NO electrical steel at different frequencies," *J. Magn. Magn. Mater.*, vol. 469, pp. 373–382, Jan. 2019, doi: 10.1016/j.jmmm.2018.07.073.

[10] F. Fiorillo, "Measurements of magnetic materials," *Metrologia*, vol. 47, no. 2, pp. S114–S142, Apr. 2010, doi: 10.1088/0026-1394/47/2/S11.

[11] E. Barbisio, F. Fiorillo, and C. Ragusa, "Predicting loss in magnetic steels under arbitrary induction waveform and with minor hysteresis loops," *IEEE Trans. Magn.*, vol. 40, no. 4, pp. 1810–1819, Jul. 2004, doi: 10.1109/TMAG.2004.830510.

[12] G. Bertotti, *Hysteresis in Magnetism*. San Diego, CA, USA: Academic Press, 1998, pp. 391–429.

[13] C. Appino, G. Bertotti, O. Bottauscio, F. Fiorillo, P. Tiberto, D. Binesti, J. P. Ducreux, M. Chiampi, and M. Repetto, "Power losses in thick steel laminations with hysteresis," *J. Appl. Phys.*, vol. 79, no. 8, pp. 4575–4577, Apr. 1996, doi: 10.1063/1.361873.

[14] S. E. Zirka, Y. I. Moroz, P. Marketos, and A. J. Moses, "A viscous-type dynamic hysteresis model as a tool for loss separation in conducting ferromagnetic laminations," *IEEE Trans. Magn.*, vol. 41, no. 3, pp. 1109–1111, Mar. 2005, doi: 10.1109/TMAG.2004.830228.

[15] L. R. Dupré, R. Van Keer, and J. A. A. Melkebeek, "Modelling and identification of iron losses in nonoriented steel laminations using Preisach theory," *Proc. Inst. Elect. Eng.-Electr., Power Appl.*, vol. 144, no. 4, pp. 227–234, Jul. 1997, doi: 10.1049/ip-epa:19971165.

[16] S. E. Zirka, Y. I. Moroz, P. Marketos, and A. J. Moses, "Congruency-based hysteresis models for transient simulation," *IEEE Trans. Magn.*, vol. 40, no. 2, pp. 390–399, Mar. 2004, doi: 10.1109/TMAG.2004.824137.

[17] O. de la Barrière, E. Ferrara, A. Magni, A. Sola, C. Ragusa, C. Appino, and F. Fiorillo, "Skin effect and losses in soft magnetic sheets: From low inductions to magnetic saturation," *IEEE Trans. Magn.*, early access, Jun. 8, 2023, doi: 10.1109/TMAG.2023.3284421.

[18] L. R. Dupre, O. Bottauscio, M. Chiampi, M. Repetto, and J. A. A. Melkebeek, "Modeling of electromagnetic phenomena in soft magnetic materials under unidirectional time periodic flux excitations," *IEEE Trans. Magn.*, vol. 35, no. 5, pp. 4171–4184, 1999, doi: 10.1109/20.799065.

[19] I. Hantila, "A method of solving stationary magnetic field in nonlinear media," *Rev. Roumaine Sci. Techn. Electr. Energ.*, vol. 20, no. 3, pp. 397–407, 1975.

[20] E. Josso, "Iron-cobalt-vanadium alloys: A critical study of the phase diagrams in relation to magnetic properties," *IEEE Trans. Magn.*, vol. MAG-10, no. 2, pp. 161–165, Jun. 1974, doi: 10.1109/TMAG.1974.1058300.

[21] F. Pfeifer and C. Radeloff, "Soft magnetic Ni-Fe and Co-Fe alloys—Some physical and metallurgical aspects," *J. Magn. Magn. Mater.*, vol. 19, nos. 1–3, pp. 190–207, Apr. 1980, doi: 10.1016/0304-8853(80)90592-2.

[22] R.C. Hall, "Magnetic anisotropy and magnetostriction of ordered and disordered cobalt-iron alloys," *J. Appl. Phys.*, vol. 31, pp. 157–158, May 1960, doi: 10.1063/1.1984643.

[23] B. E. Lorenz and C. D. Graham, "High-temperature magnetostriction in polycrystalline Fe-Co alloys," *IEEE Trans. Magn.*, vol. 40, no. 4, pp. 2751–2753, Jul. 2004, doi: 10.1109/TMAG.2004.832276.

[24] C. W. Chen, "Metallurgy and magnetic properties of an Fe-Co-V alloy," *J. Appl. Phys.*, vol. 32, no. 3, pp. 348–355, Mar. 1961, doi: 10.1063/1.2000465.

[25] *Soft Magnetic Materials and Semi-finished Products*. Accessed: Oct. 9, 2023. [Online]. Available: https://vacuumschmelze.com/03_Documents/Brochures/PHT%20001%20en.pdf

[26] Accessed: Oct. 9, 2023. [Online]. Available: https://vacuumschmelze.com/03_Documents/Brochures/Cobalt-Iron%20Alloys.pdf

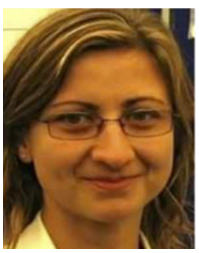

NICOLETA BANU received the joint master's degree in electrical engineering in Bucharest, in 2003, and in Grenoble, in 2004, and the Ph.D. degree in electrical engineering and in magnetism and magnetic measurements from Politecnico di Torino, in 2008. From 2009 to 2021, she was with IREM SpA in metrology and documental services. She is currently with the Laboratory for Standard Magnetic Measurements, Magnetism Group of the Materials and Life Sciences Division, Istituto Nazionale di Ricerca Metrologica (INRIM), Turin.

ENZO FERRARA received the degree in chemistry from the University of Torino, in 1989. He has been a Researcher in the field of ''materials science'' with IEN Galileo Ferraris, since 1991, now INRIM in the production research, treatment (thermal and magneto-thermal), and structural and magnetic characterization of materials used in electrical engineering (motors, transformers, actuator devices, sensors, and antennas). In the field of preparation of electromagnetic devices for high frequency applications, he has coordinated an Italy–Slovenia bilateral project ''Non-conductive magnetic materials for microwave absorbers.'' Since 1997, he has been in the field of metrology in chemistry, for the development of methods of electrochemical analysis referable to the international system (SI) of units of measurement. Eurachem Delegate (European Analytical Chemistry Forum); Delegate of working groups in electrochemical analysis of the advisory committee for quantity of substance—BIPM, Sévres (EU)—and of European Metrology in Chemistry (METCHEM). From 2003 to 2006, delegate in the ''Key Comparison and CMC Quality'' working group of the Substance Quantity Advisory Committee—BIPM, Sévres (EU). Teaching activity, since 2004, teacher of: ''Applications of magnetic measurements for artistic and cultural heritage,'' Degree Course in ''Science and Technology for Cultural Heritage,'' University of Turin. Study of the magnetic properties of natural materials, for geology and archaeology.

MASSIMO PASQUALE (Senior Member, IEEE) received the degree in particle physics from the University of Torino, in 1988. He has been a Researcher with Istituto Elettrotecnico Nazionale Galileo Ferraris, since 1991, now Istituto Nazionale di Ricerca Metrologica (INRIM), Turin. He has authored more than 100 papers on several aspects of applied magnetism, phase transitions and magnetocalorics, magnetostriction, sensors, and magnetic measurements up to the microwave regime. He has coordinated EMPIR EU projects on magnetics, including the HEFMAG Project here acknowledged and bilateral research projects with South Korea and Japan. He has served in the IEEE Magnetics Society as the Conference Chair (Intermag 2009), the Publications Chair (2010–2011), has been the Conference Publications Chair, since 2018, and the Conference Executive Committee Chair (2012–2015).

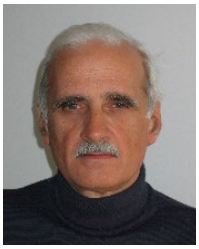

FAUSTO FIORILLO received the degree from the University of Torino, in 1972. Since 1974, he has been a scientist and since 1995, he has been the Research Director of Istituto Elettrotecnico Nazionale Galileo Ferraris, now Istituto Nazionale di Ricerca Metrologica (INRIM), Turin. He retired in January 2012. He is currently a physicist. He is also an emeritus Scientist with INRIM. His scientific work and research interests include the properties of magnetic materials and their measurement, with a focus on magnetization process and losses. He authored/coauthored some 230 peer-reviewed publications in international scientific journals, review monographs, and chapters on international series on magnetic materials. He is the author of the comprehensive treatise *Measurement and Characterization of Magnetic Materials* (10 Chapters, 647 pages) (Academic Press-Elsevier, December 2004).

OLIVIER DE LA BARRIÈRE was born in Paris, France, in 1982. He received the M.S. and Ph.D. degrees in electrical engineering from Ecole Normale Superieure de Cachan, Cachan, France, in 2007 and 2010, respectively. Since 2012, he has been a full-time Centre National de la Recherche Scientifique Researcher with the Systems and Applications of Information Technologies and Energy Laboratory (UMR8029), Gif-sur-Yvette. He was a Postdoctoral Scientist with the National Institute of Research in Metrology, Turin, Italy, in 2012. His research interests include electrical machine design, axial flux machines, and iron loss measurement and modeling in soft magnets (laminated or granular). He has been a member of the Steering Committee of Advances in Magnetics, Bormio, Italy. He has been a member or IEC committee for standardization of magnetic measurements, since 2016. He has been a member of the Steering Committee of Advances in Magnetics, Bormio, and a member or IEC committee for standardization of magnetic measurements, since 2016.

DANIEL BRUNT received the master's degree in physics from the University of Warwick, in 2013, and the Ph.D. degree from the Superconductivity and Magnetism Group, University of Warwick. The focus of his Ph.D. degree was the study of geometrically frustrated magnets, primarily through temperature and field dependent magnetic characterization and neutron scattering techniques. He is currently a Senior Scientist with NPL and since joining, in 2017, he has led various project covering the investigation of both permanent magnets and soft magnetic materials. His current research interests include developing measurement capabilities and building the metrology associated with characterization of magnetic materials at operational conditions.

ADAM WILSON received the bachelor's degree in physics from the University of Exeter and the master's degree in medical imaging from the University of Surrey. After taking a year out to work at a geotechnical firm. He was with the Electronic and Magnetic Materials Team, NPL, in November 2019. He has been involved with supporting the measurement service and research in magnetic materials characterization.

STUART HARMON is currently a Senior Scientist with the Electronic & Magnetic Materials Group with over 25 year's experience characterizing magnetic materials and sensors. He started with National Physical Laboratory working on a range of electrical measurement techniques, which then broadened to include magnetic measurements. He is involved in various research activities and is responsible for the magnetics and AC conductivity UKAS accredited (ISO 17025) measurement services. In 2016, he became the magnetics theme leader with oversight for all metrology, research, and commercial activities within the team. He chairs the BSi Committee ISE/108 and a Committee Member of IEC TC68 both titled ''Magnetic Materials and Alloys.'' He is also a Committee Secretary of SAE AE-9 for Aerospace Materials. Previously, he was a member of the U.K. Magnetics Society.

Open Access funding provided by 'Istituto Nazionale di Ricerca Metrologica - INRiM' within the CRUI CARE Agreement